

Direct Correlation Between Adhesion Promotion and Coupling Reaction at Immiscible Polymer-Polymer Interfaces

Jianbin Zhang
Phillip J. Cole
Umang Nagpal
Christopher W. Macosko

Department of Chemical Engineering and Materials Science,
University of Minnesota, Minneapolis, Minnesota, USA

Timothy P. Lodge

Department of Chemical Engineering and Materials Science and
Department of Chemistry, University of Minnesota, Minneapolis,
Minnesota, USA

*Hugh Brown has shown that interfacial entanglements govern adhesion between two polymers. We demonstrate this for three systems by adding interfacial chains via chemical coupling. The adhesion between polypropylene (PP)/amorphous polyamide (aPA) was reinforced by the coupling reaction of maleic anhydride grafted PP (PP-g-MA) and the primary amine groups on aPA; huge increases in adhesion were observed. A good correlation between critical fracture toughness, G_c , and PP-g-MA concentration squared follows Brown's crazing mechanism. For a polystyrene (PS)/aPA interface reinforced by the coupling reaction of poly(styrene-*r*-maleic anhydride) (PS-*r*-MA)/aPA only modest adhesion increases in G_c were observed through the whole PS-*r*-MA concentration range. This different behavior of G_c vs. functional polymer concentration is believed to be caused by segregation of the formed graft copolymers at the interface. The relationship between G_c and the extent of coupling was studied quantitatively with a model PS/PMMA system. The interface was reinforced by the coupling reaction of 0–10% PS-NH₂/PMMA-anh. G_c was measured with the asymmetric dual cantilever beam test*

Received 12 December 2005; in final form 9 May 2006.

One of a Collection of papers honoring Hugh R. Brown, who received *The Adhesion Society Award for Excellence in Adhesion Science*, Sponsored by 3M in February 2006.

Present address of Phillip J. Cole is: Sandia National Laboratories, Albuquerque, NM, USA.

Address correspondence to Christopher W. Macosko, Department of Chemical Engineering, University of Minnesota, Minneapolis, MN 55455, USA. E-mail: macosko@umn.edu or Timothy P. Lodge, Department of Chemistry, University of Minnesota, Minneapolis, MN 55455. E-mail: lodge@chem.umn.edu

(ADCB) and the amount of copolymer formed at the interface was determined by a fluorescence labeling technique. G_c is low and is linear in block copolymer interfacial coverage (Σ), indicating a chain scission mechanism. Reasonable agreement was achieved between experiment and theoretical prediction based on the energy to break C–C bonds.

Keywords: Adhesion promotion; Amorphous polyamide; Block copolymer; Bond energy; Critical fracture toughness; Energy to break a polymer chain; Poly(methyl methacrylate); Polypropylene; Polystyrene; Reactive coupling

INTRODUCTION

Adhesion between polymers is an important issue for polymer blends and layered polymer products [1–3]. Hugh Brown and coworkers have shown that adhesion is controlled by intermolecular chain entanglements at interfaces [4–6]. Most commercial polymer blends or layered products achieve their desired properties by combining the advantages of different polymers. Yet most of these polymer pairs are immiscible and the interface between them is narrow. This narrow interface leads to a low entanglement density across the interface that results in a weak connection between polymers [7–9].

A weak interface can limit the application of these materials. One way to enhance the strength of such an interface is to add block (or graft) polymers with each block being miscible with one of the homopolymers [10]. These copolymers can work as a molecular bridge connecting the two phases together. Depending on the molecular weight and the amount of the copolymer at an interface, different improvements in adhesion can be achieved. For example, adhesion is enhanced only modestly when the molecular weight of copolymer blocks is less than the entanglement molecular weight (M_e) of the homopolymers, independent of interfacial coverage (Σ). When the block molecular weight is higher than M_e , adhesion is a strong function of coverage. The mechanical strength of the interface can even reach that of the bulk homopolymer.

For most adhesion promotion studies premade block or graft copolymers were added to the interface by coating a copolymer layer between the two homopolymers or by premixing copolymers with one of the homopolymers [4,8,11–15]. However, premade block copolymers are not typically used to compatibilize commercial blends [16]. Instead, *in situ* copolymer formation by coupling functional polymers with complementary reactive groups is the method used in practice to control interfacial properties [16–18]. Therefore, it is important to understand the relation between interfacial adhesion and reactive coupling.

There have been many reports about promoting adhesion between immiscible polymers through *in situ* copolymer formation [19–26]. However, quantitative studies of adhesion and coupling reaction are few. The main difficulty lies in determination of the amount of copolymer formed reactively at an interface, since the total copolymer concentration is extremely low. Boucher *et al.* [20] used X-ray photoelectron spectroscopy (XPS) to detect the amount of copolymer formed by the coupling reaction between PP-g-MA/polyamide (PA) at a PP/PA interface. However, the accuracy of this method is highly dependent on how well the unreacted PA was removed from the bilayer sample without removing the PP-g-PA that was formed by reactive coupling. We have been unsuccessful in quantifying the amount of PP-g-aPA formed using XPS [27]. In this study we use a sensitive fluorescence labeling technique [28] to measure copolymer formation directly [29]. With this technique the relation between adhesion increase and coupling reaction can be studied quantitatively.

The organization of this article is as follows. First, by comparing the interfacial adhesion for two commercial systems (PP/aPA and PS/aPA) reinforced with similar coupling reactions (PP-g-MA/aPA and PS-*r*-MA/aPA) we emphasize the importance of directly correlating adhesion promotion with the extent of coupling reaction. Second, both adhesion promotion and coupling reaction were studied with a model system, amine-terminal PS (PS-NH₂)/anhydride-terminal poly(methyl methacrylate) (PMMA-anh). A direct correlation between adhesion promotion and block copolymer interfacial coverage emerged and was explained by the energy to fracture backbone bonds.

EXPERIMENTAL

Materials

The polymers used in this study are listed in Table 1. Except for the PS and PMMA functional polymers, all are commercial materials and were used as received. The molecular weight and distribution (PDI) for these polymers were either measured with size exclusion chromatography (SEC) based on PS standards or taken as given by the suppliers. The functionalities of the commercial functional polymers were given by the suppliers. The amine functionality of aPA was also measured with a fluorine nuclear magnetic resonance (NMR) technique after capping the amine group with a fluorine-containing aldehyde group [30]. The result agrees well with the value supplied by Dupont based on titration.

TABLE 1 Characteristics of Polymers Used in this Work

Polymer	Supplier	M_w (kg/mol)	M_w/M_n	f_n^*
aPA	Zytel 330 <i>Dupont</i>	50	2.0	0.6
PS	Styron 685D <i>Dow</i>	280	2.0	—
PP	MI5 <i>Huntsman</i>	120	3.0	—
PP- <i>g</i> -MA	MP320 <i>Aristech</i>	50	2.5	0.5
PS- <i>r</i> -MA	Dylark 232 <i>Nova</i>	240	2.0	96
PS-CN	Synthesized	104	1.3	—
PS-NH ₂	Synthesized	104	1.3	0.5
PMMA-anh	Synthesized	52	1.3	1.0
PMMA-anh-anth	Synthesized	43	1.3	1.0

*average number of functional units per chain based on Mn.

Dupont, Wilmington, DE, USA.

Nova Chemical, Moon Township, PA, USA.

Aristech, Florence, KY, USA.

Huntsman, Salt Lake City, UT, USA.

PS-NH₂, PMMA-anh, and anthracene-labeled PMMA-anh (PMMA-anh-anth) were synthesized by atom transfer radical polymerization (ATRP) with different functional initiators. For PS-NH₂ the initiator used was 2-bromopropionitrile and the nitrile group was reduced to an aliphatic amine end after polymerization. For PMMA-anh the initiator used was bromo-4-methylphthalic anhydride, which was made from 4-methylphthalic anhydride supplied by Avecia (Milford, MA, USA) and used as received. For PMMA-anh-anth the same initiator was used, except that an anthracene labeled methacrylate monomer was randomly incorporated into the PMMA chain with approximately one anthracene moiety per chain. All the polymerization and purification followed standard ATRP procedures for PS and PMMA. Further details of the synthesis are given elsewhere [28,31].

The molecular weight and PDI of the synthesized polymers were measured with SEC based on PS standards. The functionality of PS-NH₂ was determined by coupling it with excess PMMA-anh in dry tetrahydrofuran (THF) [31]. The reaction was brought to completion by heating the solution at 70°C for at least 24 hours and the PS-NH₂ conversion was measured with a UV detector on the SEC. The functionalities of PMMA-anh-anth and PMMA-anh were determined by coupling each of them with excess PS-NH₂ in dry THF solution at 70°C for 24 hours. The amount of coupled PMMA was measured with the fluorescence and UV detectors on the SEC, respectively.

Sample Preparation

All the polymers were dried at 80°C in a vacuum oven for at least 24 hours before use. The functional polymers were dispersed in the corresponding non-functional polymers in a batch mixer (HBI System 90, Haake, Waltham, MA, USA) with a rotor speed of 50 rpm for 10 min at different temperatures: 200°C for PP-*g*-MA/PP, 220°C for PS-*r*-MA/PS, and PS-NH₂/PS. Each of the polymers or polymer mixtures was molded into plates 2 cm wide and 7.5 cm long with a hot press. The thickness (1.0–1.8 mm) of the plate was controlled by using molds of different thickness to prepare samples suitable for the adhesion test described below. PS and PMMA samples were pressed at 220°C, while PP samples were pressed at 200°C and aPA at 240°C. Teflon[®] sheets were used to provide mold release.

Bilayer samples were prepared through melt lamination of the 2-cm by 7.5-cm plates. Two plates of different polymers were sandwiched between two stainless steel spacers and loaded into a mold with dimensions the same as the plates. The sample loading thickness can be tuned by changing the thickness of the two stainless steel spacers. The mold was then sandwiched between two backing plates and was slightly pressed (0.2 MPa) using a preheated hot press for 30 min. The temperatures used were 240°C for PP/aPA and PS/aPA and 220°C for PS/PMMA. The bilayer samples made in this way had constant layer thickness and smooth surfaces. There was no edge encapsulation. Sometimes, a small amount of polymer leaked out from the edge of the plates. The leaked-out polymer was carefully removed with a razor blade.

Adhesion Measurement

The adhesion was measured using the asymmetric dual cantilever beam crack propagation (ADCB) test. A rectangular blade of thickness Δ was driven into the interface of a bilayer sample to initiate a crack. After allowing the crack to equilibrate for half an hour, the crack length, a , was obtained with a caliper after averaging 5 measurements. Then the blade was inserted further and another crack was made.

The critical strain energy release rate or the critical interfacial fracture toughness (G_c) was quantified using the equation described by Brown and coworkers [4]:

$$G_c = \frac{3\Delta^2 E_1 E_2 h_1^3 h_2^3}{8a^4} \left[\frac{C_1^2 E_2 h_2^3 + C_2^2 E_1 h_1^3}{(C_1^3 E_2 h_2^3 + C_2^3 E_1 h_1^3)^2} \right] \quad (1)$$

where $C_i = 1 + 0.64(h_i/a)$, E_i is the modulus of component i , and h_i is the thickness of component i .

To prevent crack deviation from an interface into the plates the thickness ratio of the two polymer layers was adjusted to find the minimum G_c , which was then used to represent the true interfacial strength. The measurement was repeated on three parallel samples with 3–4 cracks for each. Thus, the reported G_c values are an average of at least 10 tests and the error bars are one standard deviation.

Conversion Measurement

PS(PS-NH₂)/PMMA-anh-anth bilayer thin films were used to measure the reaction conversion. The bilayer samples were constructed by sequentially spin-coating polymer solutions onto a silicon substrate. For example, a PMMA-anh-anth solution in toluene (*ca.* 2.0 wt%) was first spun onto a silicon wafer and dried overnight. Atomic force microscopy (AFM) indicated that the film thickness was *ca.* 30 nm. The second layer was prepared by spin-coating a PS solution (*ca.* 4.0 wt%, a mixture of PS-NH₂/PS-CN/PS) in a cyclohexane/toluene mixed solvent (87/13 v/v) onto the PMMA film. This particular mixed solvent does not dissolve the PMMA layer or perturb the interface, as verified by AFM [32–34]. Using forward recoil spectrometry (FRES), Schulze did not find any evidence of enrichment of functional groups at the interface by this sequential spin-coating process [32]. Schulze also found that reaction conversion for samples prepared by sequential spin-coating was comparable with samples prepared by spin coating a film of PMMA on a silica wafer, floating it off on water and then pressing it onto a PS layer. All these checks confirmed that sequential spin-coating does not affect the reaction conversion measurement. The bilayer samples were annealed at 220°C under nitrogen for 30 min, followed by quenching in liquid nitrogen prior to analysis.

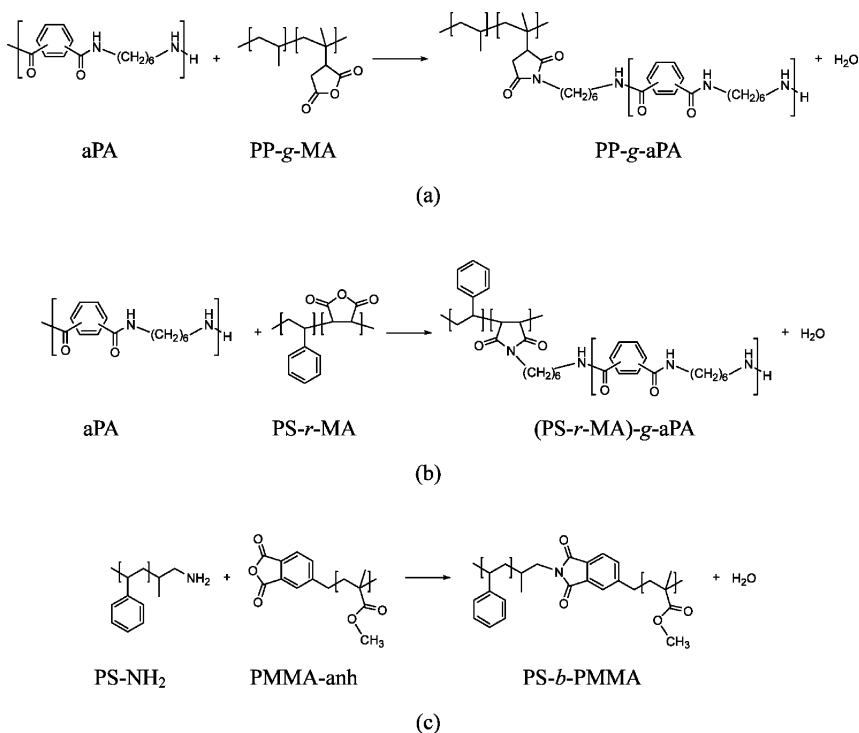
The annealed bilayer thin films were completely dissolved in about 1 mL THF. One drop of phenyl isocyanate was added to quench any unreacted amine groups. 100 μ L of the solution were then injected into a Waters 590 SEC (Milford, MA, USA) equipped with three Phenomenex PhenogelTM columns (5- μ m bead size), an internal refractive index detector (Waters 410), an external UV detector (Spectroflow 757, Kratos Analytical Instruments, Manchester, UK), and an external fluorescence detector (F-1050, Hitachi, Tokyo, Japan). The fluorescence detector was used to measure the PMMA-anh-anth conversions with excitation and emission wavelengths of 358 nm and 402 nm, respectively. The conversion of PMMA-anh-anth was extracted using peak area subtraction, as described by Jeon *et al.* [35].

RESULTS AND DISCUSSION

Adhesion Between PP/aPA and PS/aPA

As shown in Schemes 1a and 1b, both the coupling reactions used to reinforce the interfaces are between amine and anhydride groups to form an imide bond. This coupling reaction is expected to be very rapid at $T \geq 180^\circ\text{C}$ [35,36]. Therefore, the strength of these interfaces is expected to be enhanced quickly.

The adhesion between PP/aPA laminates is summarized in Figure 1(a). As the concentration of PP-g-MA in the PP layer increases, the adhesion increases tremendously. A good correlation is shown between G_c and PP-g-MA concentration squared. If the concentration of interfacial entanglements is proportional to PP-g-MA concentration, then this squared dependence indicates failure by crazing [5]. The extremely high adhesion ($>100\text{ J/m}^2$)



SCHEME 1 Coupling reaction between (a) PP-g-MA/aPA; (b) PS-r-MA/aPA; and (c) PS-NH₂/PMMA-anh.

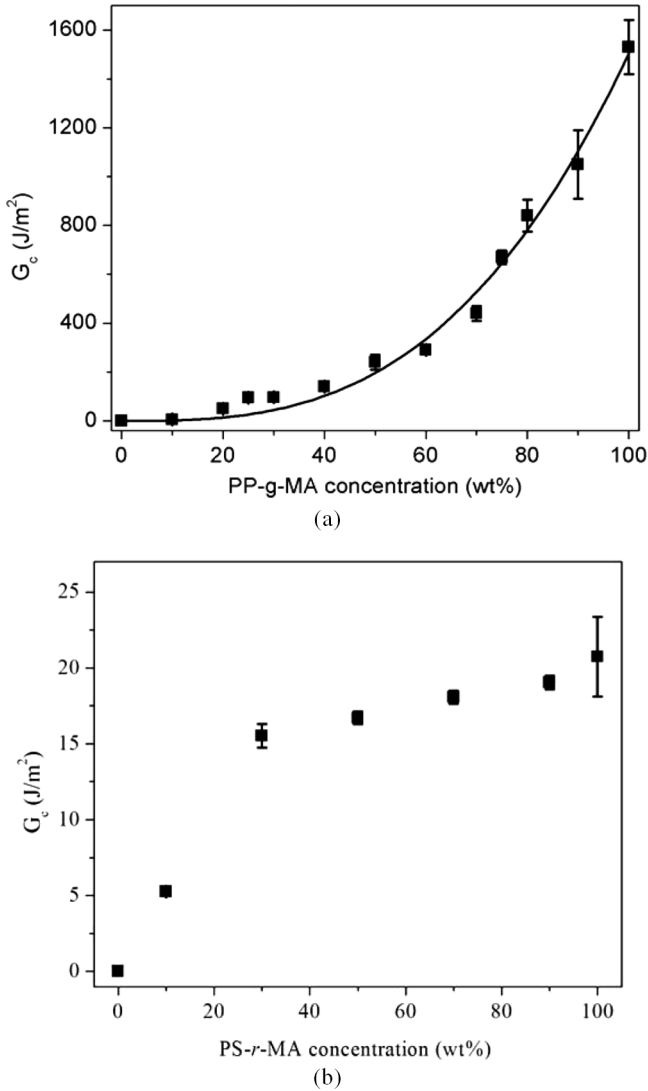


FIGURE 1 G_c vs. functional polymer concentration for (a) PP/aPA reinforced by the coupling reaction between PP-g-MA/aPA. The solid line is the 2nd power fitting of G_c vs. PP-g-MA concentration; (b) PS/aPA reinforced by the coupling reaction between PS-r-MA/aPA.

achieved also suggests that cocrystallization of PP and the PP blocks in PP-g-aPA plays an important role in enhancing the interfacial strength [37].

For the PS/aPA system the situation is quite different. As shown in Figure 1(b), G_c is much lower than that for PP/aPA. A modest increase in adhesion was observed on increasing the PS-*r*-MA concentration to 30 wt%, but further increasing PS-*r*-MA concentration did not change the adhesion much, even for pure PS-*r*-MA/aPA. Similar results were reported by Lee *et al.* [24] and Cho *et al.* [25]. Considering that both PP/aPA and PS/aPA were reinforced with the same coupling reaction, the large difference in adhesion is surprising. One can argue that the low miscibility between PS/PS-*r*-MA causes less reaction at the PS/aPA interfaces. However, this effect does not account for the low adhesion obtained for pure PS-*r*-MA/aPA. Lee *et al.* argued that for PS-*r*-MA/aPA, the extreme asymmetry on stoichiometry between anhydride and amine groups (96:0.6) leads to a highly grafted PS-*g*-aPA being formed. The copolymers stay at the interface as a separated phase and have low entanglement with the homopolymers, which results in poor adhesion.

The results for these two systems indicate that adhesion is not controlled directly by the concentration of functional polymers, but rather by the amount and the architecture of copolymer formed at an interface. For these two systems it is hard to measure conversion and, thus, difficult to correlate the adhesion increase with the extent of the coupling reaction. Therefore, we designed a PS-NH₂/PMMA-anh model system (with the same coupling chemistry, as shown in Scheme 1c) to permit measurement of both adhesion and the amount of block copolymer.

Model System PS/PMMA

The molecular weights of both PS-NH₂ and PMMA-anh are above M_e for the corresponding homopolymers. Thus, the interfaces between PS/PMMA reinforced by the coupling reaction of PS-NH₂/PMMA-anh will fracture through the chain-scission/crazing mechanism. The critical block copolymer interfacial coverage (Σ_c) for the transition of the fracture mechanism from chain scission to crazing can be estimated by Equation (2) [10]:

$$\Sigma_c = \frac{\sigma_{cr}}{f_b} \quad (2)$$

where σ_{cr} is the crazing stress of the homopolymer and f_b is the force required to break a main-chain bond (carbon-carbon bond here). The crazing stresses for PS and PMMA are 55 and 70 MPa, respectively, and f_b is *ca.* 1.9×10^{-9} N [10]. Therefore, the relevant Σ range we will focus on is $\Sigma_c \approx 0.03$ chain/nm².

In a separate study we have shown that the amount of copolymer formed at a PS/PMMA interface by the same coupling reaction can be

quantitatively controlled by adjusting PS-NH₂ concentration in the PS layer, while keeping the PMMA layer pure PMMA-anh [31]. It was found that when the PS-NH₂ concentration is ~10 wt%, Σ will be around Σ_c . Therefore, the PS-NH₂ concentration used here is between 0–10 wt% and the PMMA layer is pure PMMA-anh. Because the functionality of PS-NH₂ is 0.5 the maximum amount of low molecular weight PS dispersed in the high molecular weight matrix is 20 wt%. To maintain the same level of low molecular weight polymer in the PS layer a complementary amount of nonfunctional PS (PS-CN) with the same molecular weight was added when the PS-NH₂ concentration went down.

Figure 2 shows that the adhesion increases with PS-NH₂ concentration. Because the amine concentration was intentionally kept low the PS/PMMA interfacial strength was enhanced only modestly.

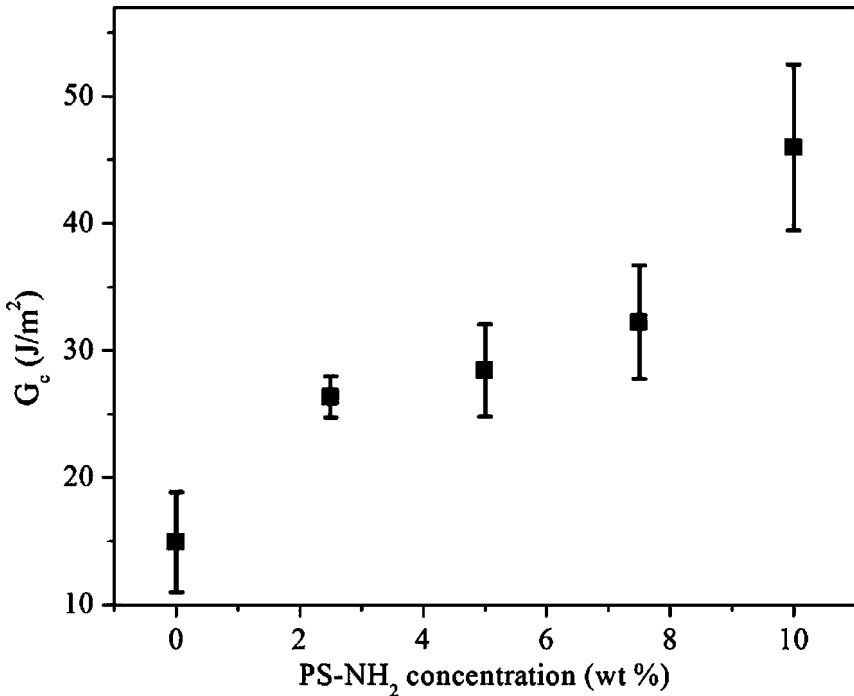


FIGURE 2 G_c vs. PS-NH₂ concentration for the PS/PMMA system. The PMMA layer is pure PMMA-anh, while the PS layer is a mixture of PS-NH₂/PS-CN/PS. In the PS layer Styron 685D was kept at 80 wt%, while the remaining 20 wt% was a mixture of PS-CN/PS-NH₂ to maintain the same level of low molecular weight PS in the PS layers for all the PS-NH₂ concentration.

For conversion measurements a bilayer sample of PMMA-anh-anth with similar molecular weight to PMMA-anh was used. The thickness of the PMMA layer was around 30 nm, which facilitated the detection of the small amount of block copolymer formed at low PS-NH₂ concentration while still keeping PMMA-anh-anth the majority reactant compared with PS-NH₂. The layer thickness has been proven not to affect the amount of copolymer formed at an interface [31,34,35,38]. As discussed below, the amount of block copolymer formed here is consistent with the results we achieved with a 150-nm-thick PMMA layer [31]. For the same reason it allows us to use the conversions measured for the spin-coated bilayers to access that of the laminated bilayers.

The PMMA-anh-anth conversion increases with PS-NH₂ concentration, as shown in Figure 3. From PMMA-anh-anth conversion Σ can be calculated from layer thickness with Equation (3), assuming that a flat interface was still maintained after annealing:

$$\Sigma = \frac{l\alpha\rho N_{AV}}{M_n} \quad (3)$$

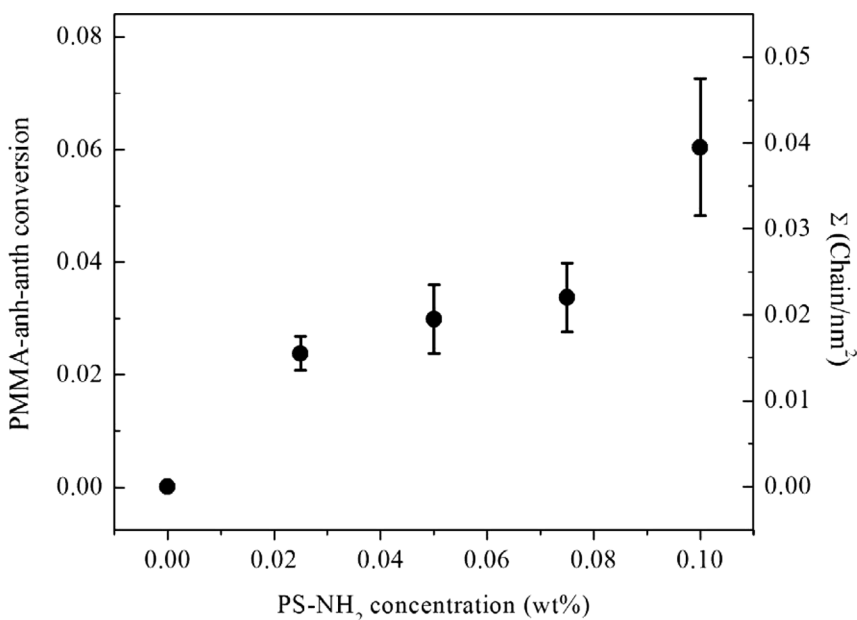


FIGURE 3 PMMA-anh-anth conversion (left axis) *vs.* PS-NH₂ concentration from annealing of spin-coated bilayer samples at 220°C for 30 min. The block copolymer interfacial coverage (right axis), Σ , was calculated from the PMMA-anh-anth conversion and layer thickness by Equation (3).

Here l is the thickness of the PMMA-anh-anth layer, ρ , α , and M_n are the density, the conversion, and the number average molecular weight of PMMA-anh-anth, respectively, and N_{AV} is Avogadro's number. Σ vs. PS-NH₂ concentration is also plotted in Figure 3. At PS-NH₂ = 10 wt%, Σ is comparable with our previous results [31] and is approximately Σ_c .

The fraction of interface covered by block copolymers can be calculated by comparing Σ with the maximum interfacial coverage (Σ^*) at a PS/PMMA interface, which can be estimated by assuming a dense monolayer of block copolymer at the interface. The thickness of this hypothetical monolayer is half of the lamellar spacing in the corresponding ordered block copolymer phase. Thus, the maximum interfacial coverage can be estimated by Equation (4).

$$\Sigma^* = \frac{\text{thickness of copolymer monolayer}}{\text{volume of one chain}} \quad (4)$$

Using the empirical relationship developed by Russell *et al.* based on neutron reflectivity experiments [39], Σ^* is estimated to be *ca.* 0.13 chain/nm² for the PS-*b*-PMMA copolymer formed here. Compared with Σ^* , all the interfaces studied here are unsaturated.

Correlation Between G_c and Σ

With this model PS/PMMA system G_c and Σ can be directly correlated. As shown in Figure 4, G_c increases linearly with Σ . This is consistent with the chain-scission fracture mechanism (Equation (2)) [10]. However, because we measure G_c instead of σ it will be more straight forward to relate G_c to Σ through an energy parameter.

The way we proposed to understand the relationship between G_c and Σ starts from the energy to break a carbon-carbon bond, U_b , instead of f_b . As shown by the cartoon in Figure 5, before fracture, block copolymers are randomly distributed along the interface. When a crack is developed, the fracture energy at the crack tip is dissipated partially by the intermolecular entanglements between the two homopolymers and by the block copolymer bridges. The fracture energy contribution from intermolecular entanglements is assumed to be the same as the homopolymer interfaces. Thus, the fracture energy increase in the chain scission regime is exclusively from broken copolymer bridges, which is directly proportional to Σ and the energy to break a block copolymer chain (U). Therefore, the fracture toughness of a reinforced interface can be expressed by:

$$G_c = G_{c0} + U\Sigma \quad (5)$$

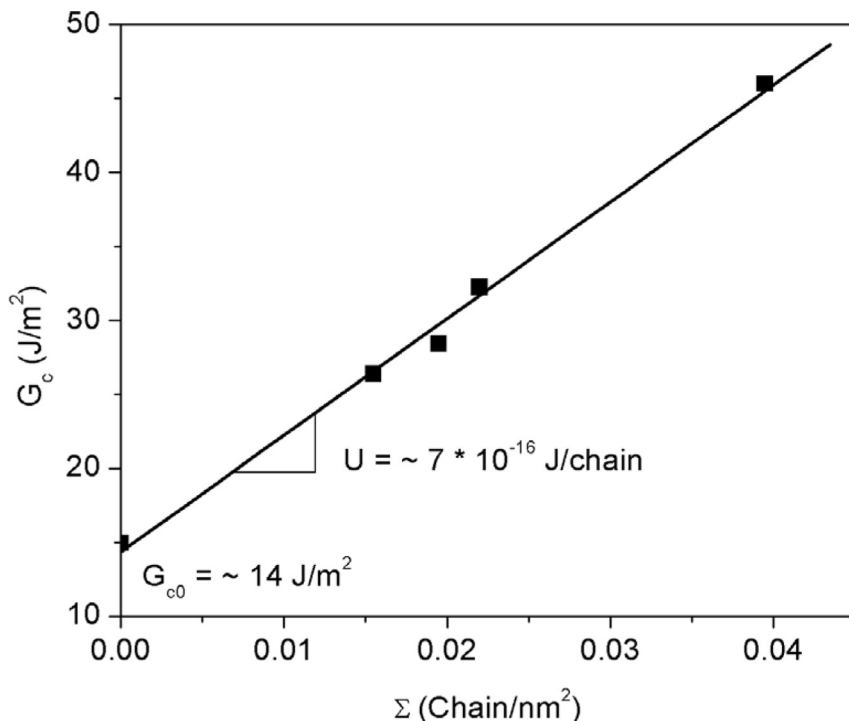


FIGURE 4 G_c increases linearly with interfacial coverage, Σ , for the PS/PMMA interface reinforced with PS-*b*-PMMA at low Σ .

where G_{c0} is the fracture toughness of the unmodified interface between the two homopolymers. From Figure 4, G_{c0} is $\sim 14 \text{ J/m}^2$, in fair agreement with Brown [14] and Cole [9] ($12 \pm 2 \text{ J/m}^2$). From the slope in Figure 4, the energy to break a PS-*b*-PMMA chain is $\sim 7 \times 10^{-16} \text{ J/chain}$.

The fracture energy dissipated by block copolymers is distributed along the carbon-carbon bonds of the block polymer chain, as shown in Figure 5. However, this energy is only dissipated on the backbone carbon-carbon bonds between the two entanglements formed by the copolymer blocks and the corresponding homopolymers that are closest to the junction between the copolymer blocks. Assuming the energy is uniformly distributed among these carbon-carbon bonds, fracture will happen when the energy dissipated by one carbon-carbon bond exceeds $U_b \cong 6 \times 10^{-19} \text{ J/bond}$. Thus, the maximum energy that can be dissipated by an entangled block copolymer chain, *i.e.*, the energy needed to break a block copolymer chain, can be estimated by:

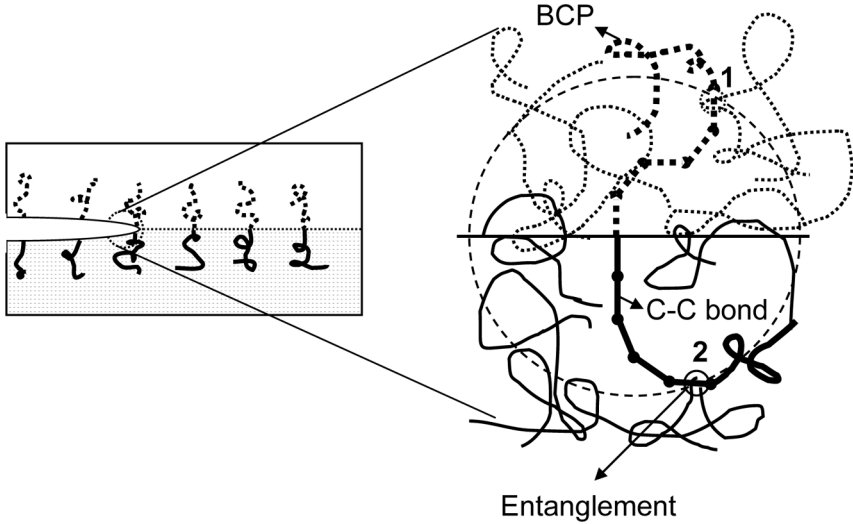


FIGURE 5 A schematic drawing shows the proposed fracture mechanism at an interface reinforced by block copolymers. The fracture energy is partially dissipated among the carbon-carbon bonds of the copolymer chain between the entanglements (1 and 2) of copolymer blocks with the corresponding homopolymers.

$$U_{\max} = U_b(n_A N_{eA} + n_B N_{eB}) \quad (6)$$

where n_i is the number of carbon bonds per i monomer and N_{ei} is the entanglement molecular weight (in terms of degree of polymerization) for i . Clearly, U_{\max} is independent of block copolymer molecular weight. For PS-*b*-PMMA $n_A = n_B = 2$, $N_{ePS} = 130$, and $N_{ePMMA} = 100$ [40]; therefore, $U_{\max} \cong 3 \times 10^{-16}$ J/chain. This predicted energy to break a chain is reasonably consistent with the experimental value for U (7×10^{-16} J/chain). Considering that a block copolymer chain at an interface is stretched, the chain length between entanglements will be higher than N_e for homopolymers. Therefore, U_{\max} calculated here is an underestimate. At the same time the coexistence of some plastic deformation even at low Σ also would result in a higher measured U .

Assuming the energy to break a PS-*g*-aPA chain is the same as that for PS-*b*-PMMA, Σ for the PS-*r*-PMMA/aPA system can be estimated to be around 0.03 chain/nm² from Figure 1(b). Clearly, for this system, even though many copolymer chains could possibly be formed at the interface, those working as effective connections between the two phases are much less due to the high grafting density.

So far, all the quantitative analysis is based on the PS/PMMA model system with low interfacial coverage. Chain scission dominates the fracture in this region. As the coupling reaction goes further, interfacial strength will be enhanced more and fracture will transit to crazing. Crazing is much more complex than scission making application of this simple energy model more difficult.

CONCLUSIONS

The interfaces between PP/aPA and PS/aPA fractured differently even though both were reinforced by an amine/anhydride coupling reaction. Tremendous increases on adhesion were found for the PP/aPA interfaces, and G_c increases with PP-*g*-MA concentration squared, indicating failure by crazing. In contrast, for PS/aPA only a small increase was observed through the whole PS-*r*-MA concentration range. This large difference in adhesion promotion was believed to be caused by the amount and the architecture of the copolymer at the interface.

A PS/PMMA model system allows measurement of Σ and G_c simultaneously. A linear relationship between G_c and Σ was confirmed and from the slope the energy needed to break a copolymer chain (U) was extracted. A chain fracture mechanism was proposed and U was also calculated from the carbon-carbon bond energy. Reasonable agreement was achieved between the experimental value (7×10^{-16} J/chain) and the theoretical prediction (3×10^{-16} J/chain).

ACKNOWLEDGMENTS

This research has been supported in part by the MRSEC program of the National Science Foundation under Award Number DMR-0212302 and IPRIME (the Industrial Partnership for Research in Interfacial and Materials Engineering) at the University of Minnesota.

REFERENCES

- [1] Brown, H. R., *Annu. Rev. Mater. Sci.* **21**, 463–489 (1991).
- [2] Brown, H. R., *Mater. Res. Soc. Symp. Proc.* **264**, 183–198 (1992).
- [3] Wu, S., *Polymer Interfaces and Adhesion* (Marcel Dekker, Inc., New York, 1987), Ch. 10, p. 337.
- [4] Creton, C., Kramer, E. J., Hui, C. Y., and Brown, H. R., *Macromolecules* **25**, 3075–3088 (1992).
- [5] Brown, H. R., *Macromolecules* **24**, 2752–2756 (1991).
- [6] Silvestri, L., Brown, H. R., Carra, S., and Carra, S., *J. Chem. Phys.* **119**, 8140–8149 (2003).

- [7] Brown, H. R., *Macromolecules* **34**, 3720–3724 (2001).
- [8] Schnell, R., Stamm, M., and Creton, C., *Macromolecules* **31**, 2284–2292 (1998).
- [9] Cole, P. J., Cook, R. F., and Macosko, C. W., *Macromolecules* **36**, 2808–2815 (2003).
- [10] Creton, C., Kramer, E. J., Brown, H. R., and Hui, C. Y., *Adv. Polym. Sci.* **156**, 53–136 (2001).
- [11] Benkoski, J. J., Flores, P., and Kramer, E. J., *Macromolecules* **36**, 3289–3302 (2003).
- [12] Bernard, B., Brown, H. R., Hawker, C. J., Kellock, A. J., and Russell, T. P., *Macromolecules* **32**, 6254–6260 (1999).
- [13] Brown, H. R., *Macromolecules* **22**, 2859–2860 (1989).
- [14] Brown, H. R., Char, K., and Deline, V. R., *Macromolecules* **26**, 4155–4163 (1993).
- [15] Reichert, W. F. and Brown, H. R., *Polymer* **34**, 2289–2296 (1993).
- [16] Koning, C., Van Duin, M., Pagnouille, C., and Jérôme, R., *Prog. Polym. Sci.* **23**, 707–757 (1998).
- [17] Paul, D. R. and Bucknall, C. B., *Polymer Blends* (Wiley, New York, 2000), Vol. 2, Ch. 23, p. 119.
- [18] Macosko, C. W., Jeon, J. K., and Hoyer, T. R., *Prog. Polym. Sci.* **30**, 939–947 (2005).
- [19] Beck Tan, N. C., Peiffer, D. G., and Briber, R. M., *Macromolecules* **29**, 4969–4975 (1996).
- [20] Boucher, E., Folkers, J. P., Hervet, H., Léger, L., and Creton, C., *Macromolecules* **29**, 774–782 (1996).
- [21] Laurens, C., Creton, C., and Léger, L., *Macromolecules* **37**, 6814–6822 (2004).
- [22] Norton, L. J., Smigolova, V., Pralle, M. U., Hubenko, A., Dai, K. H., Kramer, E. J., Hahn, S., Berglund, C., and DeKove, B., *Macromolecules* **28**, 1999–2008 (1999).
- [23] Cole, P. J. and Macosko, C. W., *J. Plastic Film Sheeting* **16**, 213–222 (2000).
- [24] Lee, Y. and Char, K., *Macromolecules* **27**, 2603–2606 (1994).
- [25] Cho, K., Seo, K. H., and Ahn, T. O., *J. Appl. Polym. Sci.* **68**, 1925–1933 (1998).
- [26] Lu, Q., Macosko, C. W., and Horrión, J., *J. Polym. Sci. Polym. Chem.* **43**, 4217–4232 (2005).
- [27] Cole, P. J., *Polymer-Polymer Adhesion in Melt-Processed Multilayered Structure*, (Ph.D Thesis, University of Minnesota, 2002).
- [28] Moon, B., Hoyer, T. R., and Macosko, C. W., *Polymer* **43**, 5501–5509 (2002).
- [29] Schulze, J. S., Moon, B., Hoyer, T. R., Macosko, C. W., and Lodge, T. P., *Macromolecules* **34**, 200–205 (2001).
- [30] Ji, S., Hoyer, T. R., and Macosko, C. W., *Macromolecules* **38**, 4679–4686 (2005).
- [31] Zhang, J., Lodge, T. P., and Macosko, C. W., *Macromolecules* **38**, 6586–6591 (2005).
- [32] Schulze, J., *Reaction Kinetics of End-Functionalized Chains at Polymer-Polymer Interfaces*, (Ph.D Thesis, University of Minnesota, 2001).
- [33] Schulze, J. S., Cernohous, J. J., Hirao, A., Lodge, T. P., and Macosko, C. W., *Macromolecules* **33**, 1191–1198 (2000).
- [34] Yin, Z., Koulic, C., Pagnouille, C., and Jérôme, R., *Langmuir* **19**, 453–457 (2003).
- [35] Jeon, H. K., Macosko, C. W., Moon, B., Hoyer, T. R., and Yin, Z., *Macromolecules* **37**, 2563–2571 (2004).
- [36] Orr, C., Cernohous, J., Guégan, P., Hirao, A., Jeon, H. K., and Macosko, C. W., *Polymer* **42**, 8171–8178 (2001).
- [37] Boucher, E., Folkers, J. P., Creton, C., Hervet, H., and Léger, L., *Macromolecules* **30**, 2102–2109 (1997).
- [38] Jones, T. D., Schulze, S., Macosko, C. W., Moon, B., and Lodge, T. P., *Macromolecules* **36**, 7212–7219 (2003).
- [39] Anastasiadis, S., Russell, T., Satija, S., and Majkrzak, S., *J. Chem. Phys.* **92**, 5677–5691 (1990).
- [40] Fetters, L. J., Lohse, D. J., Richter, D., Witten, T. A., and Zirkel, A., *Macromolecules* **27**, 4639–4647 (1994).